Article

Preparation of Butadiene-Bridged Polymethylsiloxane/Ethylcellulose/1-Carboxymethyl-3-methylimidazolium Chloride Ternary Composite Membranes for Gas Separation

Wenqiang Ma, Shuangping Xu,* Hongge Jia,* Jingyu Xu,* Da Liu, Mingyu Zhang, Yanqing Qu, Hailiang Zhou, Yushu Zhang, Xintian Wang, and Wenwen Zhao

Read Online

ACCESS | Metrics & More | Article Recommendations | Supporting Information

ABSTRACT: Excessive CO_2 emissions have resulted in global warming and are a serious threat to the life of people, various strategies have been implemented to cut carbon emissions, and one of them is the use of a gas separation membrane to capture CO_2 effectively. In this experiment, the butadiene-bridged polymethylsiloxane (BBPMS)/ethyl cellulose (EC)/ionic liquid (IL) ternary composite membranes were prepared by EC as a substrate, BBPMS, and IL as additives in tetrahydrofuran under high-speed stirring and coated on the membrane. The membrane structure was characterized by a Fourier transform infrared spectrometer and scanning electron microscope, and the membrane properties were tested by a membrane tensile strength tester, thermal weight loss analyzer, and gas permeability meter. The results show that the surface of the ternary composite membrane is dense and flat with a uniform distribution, and the membrane formation, heat resistance, and mechanical properties are good. The

permeability coefficient of the ternary composite membrane for CO_2 reached 1806.03 Barrer, which is 20.00 times higher than that of the EC/IL hybrid matrix membrane. The permeability coefficient of O_2 reached 321.01 Barrer, which is 19.21 times higher than that of the EC/IL membrane. When the doping amount of BBPMS is 70−80%, the O_2/N_2 gas permeation separation of the BBPMS/EC/IL ternary composite membrane is close to the Robertson 2008 curve. It is always known that in the gas separation process the membrane material is the most crucial factor. The success of this experiment points to a new direction for the preparation of new membrane materials.
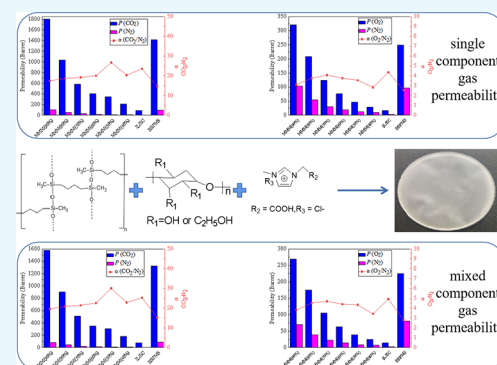
1. INTRODUCTION

As a major greenhouse gas, the increasing amount of CO_2 in the atmosphere and oceans is not only contributing to global warming and climate change but is also having a significant impact on the growth of some plants and microorganisms.[1] On the other hand, as an abundant and readily available non-toxic carbon resource, CO_2 has been used as an important feedstock for the production of chemicals, fuels, and polymers.[2] Therefore, effective, simple, and cost-effective separation and capture of carbon dioxide is important for reducing the greenhouse effect and utilizing carbon resources.[3−5]

Carbon dioxide separation and capture technologies mainly include temperature swing adsorption technology,[6] porous solid adsorption,[7] and membrane separation.[8−10] Among them, the membrane separation methods are widely used for their economic, efficient, and convenient advantages.[11,12] The separation of gases, such as CO_2/CH_4, CO_2/N_2, and O_2/N_2 by membrane separation methods, has a history of being used for several decades.[13] Various polymeric materials with excellent formability and tunable properties, such as ethyl cellulose (EC), silicone rubber, polyolefins, polyimides, and polysulfone, have been widely used as membrane materials for

gas separation.[14−16] EC is produced using natural cellulose and has good membrane making properties, high tensile strength, and carbon dioxide as well as oxygen selectivity; therefore, it occupies an important position in the field of carbon dioxide and oxygen separation.[17] However, the carbon dioxide permeability coefficient of the pure membrane of ethylcellulose is not high and to improve the gas separation performance, modification or co-blending of ethylcellulose is a good method, by adding various carbon-based hybrid matrix materials such as zeolites,[18] silica,[19] carbon nanotubes,[20] titanium dioxide,[21] and ionic liquids (IL).[22] Although these methods can increase the permeability or/and selectivity of CO_2, their increment is limited due to poor compatibility and a non-uniform distribution. Therefore, it is still important to develop high-
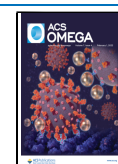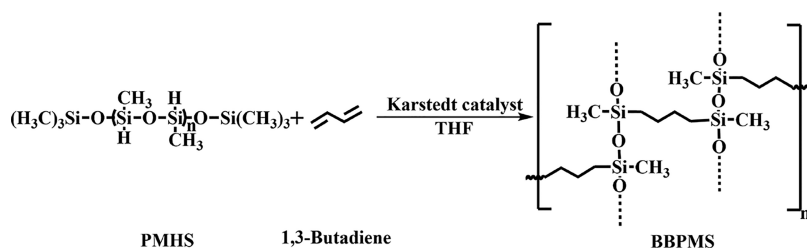
Scheme 1. Synthesis of Butadiene-Bridged BBPMS

performance polymeric gas separation membrane materials with high gas separation performance, good stability, mechanical properties, durability, easy preparation process, and low cost.

In recent years, research on the application of polysiloxanes in the direction of gas separation membranes has become more and more extensive,[23] but little research has been reported on the use of diene-based compounds bridged with polymethylhydrosiloxanes (BBPMS). Diene-bridged polymethylsiloxane has become an important research direction for gas separation membrane materials due to its many unique features, such as simple reaction conditions, high gas permeability, low cost input, and high structural variability.[24,25]

EC as an abundantly available, renewable, and low cost non-ionic cellulose ether was used in a lot of fields, such as food, filtration, microencapsulation, and medicine.[26] Remarkably, EC with a large number of ethyl groups and the unsubstituted hydroxyl groups resulted in it possessing easy film formation[27] and good gas separation performance.[28,29]

In order to further broaden the research of EC as gas separation membrane materials, this paper is based on the groups' previous adequate research on the blended membrane of 1-carboxymethyl-3-methylimidazolium chloride salt (IL) and EC.[26] A series of butadiene-bridged BBPMS/EC/1-carboxymethyl-3-methylimidazolium chloride (IL) composite membranes with butadiene-bridged BBPMS contents of 40, 50, 60, 70, 80, and 90% were prepared by incorporating polysiloxane. The structural, mechanical, and thermal properties were characterized and tested, and a series of hybrid matrix membranes were focused on O_2/N_2 and CO_2/N_2 permeation performance and separation selection performance. It is always known that in the gas separation process, the membrane material is the key factor.[30] In this paper, we propose and prepare an effective and simple EC-based gas separation membrane with preferential permeability to carbon dioxide. Successful preparation of new membrane materials opens up new paths for the development of separation membranes.

2. EXPERIMENTAL SECTION

2.1. Materials. EC was purchased from Chembee (Shanghai, China). The EC (M70) was 40−100 MPa·s, 95% pure, and contained 5% toluene/isopropanol = 80:20. PMHS and Karstedt's catalyst were purchased from Kejunchi Technology Co. (Shenzhen, China). 1-Carboxymethyl-3-methylimidazole chloride salt (IL) was purchased from Aulico New Material Technology Co. (Qingdao, China). Butadiene was purchased from Inokai Technology Co. (Beijing, China). Tetrahydrofuran (THF) was purchased from Comio Chemical Reagent Co. (Tianjin, China), the THF is analytically pure, 98% purity.

2.2. Preparation of Butadiene-Bridged BBPMS. According to Scheme 1, a three-necked flask was evacuated

for 10 min and flushed with nitrogen. Then, 5 mL of butadiene (approximately 15% of hexane), 0.1 mL of the Karstedt's catalyst, and 10 mL of THF were added to a three-necked flask. The mixture was stirred at 85 °C for 1 h. Subsequently, 1 mL of PMHS was added and stirred for another 4 h to obtain a colorless and clear solution.

2.3. Preparation of BBPMS/EC/IL Ternary Blended Membrane. EC (1.80 g, 7.58 mmol) and THF (20 mL) were placed in a flask and stirred at high speed. After the EC was completely dissolved, a well-mixed methanol solution containing 1-carboxymethyl-3-methylimidazolium chloride salt (IL) (8%, 156.52 mg) was added, and then the reaction was continued for 2 h to obtain EC (IL: 8 wt %) homogeneous solution. The reaction was carried out at room temperature.

The BBPMS synthesized in Materials section was added to an EC (IL: 8 wt %) homogeneous solution and continued to react for 1 h at room temperature to obtain a homogeneous cast membrane solution; the cast membrane solution was filtered through a 200 mesh filter and then the membrane was spread on a clean glass plate and dried naturally at room temperature for 12 h. After 12 h of vacuum drying at room temperature, the membrane was removed from the glass plate to obtain a BBPMS/EC/IL ternary composite membrane. The composite membrane composition of this study is shown in Table 1.

Table 1. Composition of Composite Membranes

no.	sample	BBPMS addition amount (mL)	BBPMS/loading[a] (wt %)	composite membranes/matrix[b] (wt %)
1	IL/EC	0.00	0.00	100.00
2	BBPMS	30.00	100.00	0.00
3	MMM(40%)	1.30	40.00	60.00
4	MMM(50%)	1.90	50.00	50.00
5	MMM(60%)	2.80	60.00	40.00
6	MMM(70%)	4.40	70.00	30.00
7	MMM(80%)	7.50	80.00	20.00
8	MMM(90%)	16.90	90.00	10.00

[a]Mass fraction of BBPMS in the composite membrane. [b]Mass fraction of EC (IL: 8 wt %) in the composite membrane.

2.4. Measurements. A Fourier transform infrared (FTIR) spectrometer (Spectrum Two, PE company, Waltham, Massachusetts, USA) was used to characterize the molecular structures of the functional groups in mixed matrix membranes. The surface structure of gas separation membranes were studied by scanning electron microscopy (SEM, JSM-6490, JOEL, Japan). The thickness of the membranes was measured by a thickness gauge (CH-1-B, Liuling Instrument Factory, Shanghai, China). The graduation value was 0.001 mm, the measurement range was 0−1 mm, and the error was

about ≤0.007 mm. Mechanical properties were analyzed with a membrane tensile testing machine (XLW(PC)−500N, Sumspring, Jinan, China) at 25 °C. A thermogravimetric analyzer (Q5000IRS type, American TA Co., Ltd., USA) was used to test the thermal performance of the membranes. During the test, the membranes were heated to 550 °C. The pure gas permeation property tests were performed using a fixed-volume pressure increase instrument time-lag apparatus (VAC-V2 type, Labthink instrument Co., Ltd, Jinan, China) at 34 °C. The membranes were first placed in a stainless-steel cell, and the disk was sealed with rubber O-rings to avoid leakage. Then, both the upstream and downstream sides of the system were degassed at ambient temperature to ensure that the system was not disturbed. Next, pure gases (CO_2, O_2, and N_2) were fed into the membrane individually, and the permeability of each pure gas was measured at a feed pressure of 2 bar. The permeability coefficients of the mixed gas were measured by a gas chromatographic method using a differential pressure gas transmission instrument (GTR-11MH type) at 34 °C.[31]

3. RESULTS AND DISCUSSION

3.1. Infrared Analysis of Membranes. The peaks and absorption bands of components in the obtained ternary composite membranes were observed and assigned by FTIR spectrometry. Judging from Figure 1, the two weak spectral
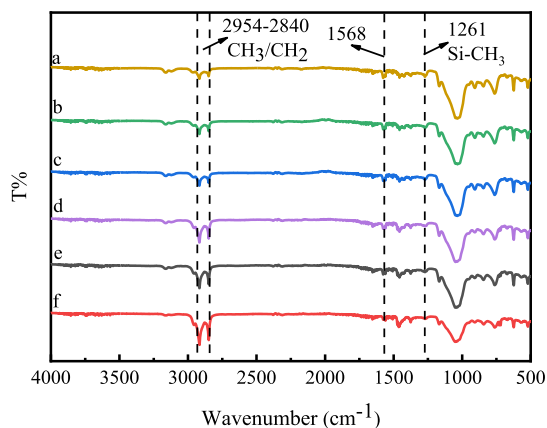

Figure 1. FTIR spectrum of the ternary composite membrane [(a): MMM(90%), (b): MMM(80%), (c): MMM(70%), (d): MMM(60%), (e): MMM(50%), and (f): MMM(40%)].

bands of 2954 and 2840 cm^{-1} belong to the C−H bond stretching vibration of methyl and methylene groups in EC, respectively. The Si−CH_3 absorption peak of BBPMS appears at 1261 cm^{-1}. However, the Si−H characteristic absorption peak of BBPMS does not appear at 2165 cm^{-1}, probably because the double bond in 1-carboxymethyl-3-methylimidazolium chloride (IL) reacts with the Si−H bond, making the Si−H bond completely reacted. The absorption peak at 1568 cm^{-1} originates from the vibration of the imidazole ring skeleton. Therefore, it can be proved that the presence of IL, EC, and BBPMS in the mixed matrix membrane, and the gradual decrease of the methyl/methylene peak in the IR spectrum with the gradual increase of the doping amount of BBMPS, proves that the amount of EC gradually decreases, which is also consistent with the doping ratio of the composite membrane.

FTIR was used to verify the change of the double bond of the EC, IL, BBPMS, and ternary composite membrane

(because the IR images of different scales of ternary composite membranes are similar, they are referred to by the same curve). As shown in Figure 2, the C═C characteristic absorption peak
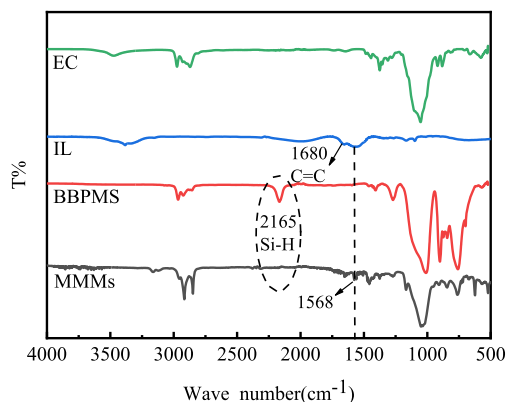

Figure 2. FTIR spectrum of the EC, IL, BBPMS, and ternary composite membrane.

of IL does appear at 1680 cm^{-1} and the Si−H characteristic absorption peak of BBPMS does appear at 2165 cm^{-1}. Both the C═C double bond and Si−H are missing in the final ternary composite membranes, which proves the successful reaction of IL with BBPMS.

3.2. SEM Analysis of Membranes. Figure 3 gives the optical pictures of the EC/IL membrane and the BBPMS/EC/
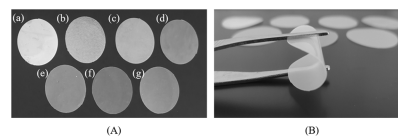

Figure 3. Optical photos [(A) transparency of the membrane varies with the amount of BBMPS doping and (B) flexibility of the membrane] of the EC/IL membrane (g) and BBPMS/EC/IL mixed matrix membranes [(a): MMM(90%), (b): MMM(80%), (c): MMM(70%), (d): MMM(60%), (e): MMM(50%), and (f): MMM(40%)].

IL ternary composite membranes. Compared to the colorless and transparent EC/IL membrane, the ternary composite membrane become less and less transparent as BBPMS increases. However, the ternary composite membranes also show the same excellent flexibility with repeated curling without deformation or breakage as the EC/IL membrane.

To further observe the distribution of BBPMS in the ternary composite membranes by SEM analysis. Figure 4 gives the surface SEM images of the EC/IL membrane (g), (h) pure BBPMS, and BBPMS/EC/IL ternary composite membranes [(a): MMM(90%), (b): MMM(80%), (c): MMM(70%), (d): MMM(60%), (e): MMM(50%), and (f): MMM(40%)]. According to Figures 4 and S1, the surface of EC/IL membrane is dense, flat and smooth. Compared with the EC/IL membrane, the surface changes of the BBPMS/EC/IL ternary composite membranes became more and more obvious with the increase of BBPMS content.However, the surface of the membranes were still uniformly distributed without agglomeration, indicating that homogeneous ternary composite membranes of EC-doped BBPMS and IL were successfully prepared.
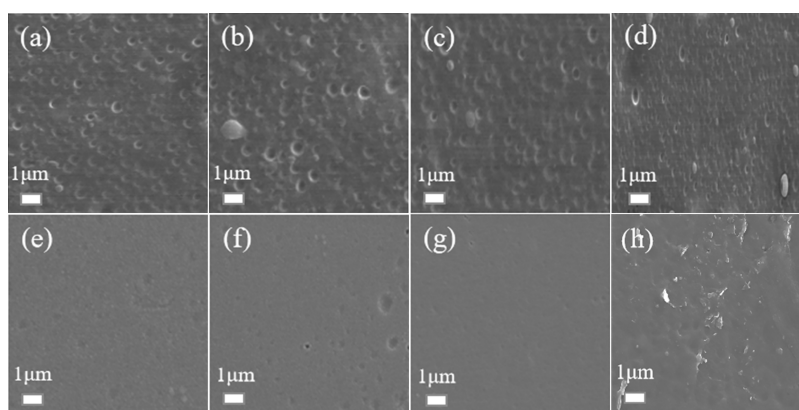
Figure 4. Surface SEM images of the EC/IL membrane (g) and BBPMS/EC/IL mixed matrix membranes [(a): MMM(90%), (b): MMM(80%), (c): MMM(70%), (d): MMM(60%), (e): MMM(50%), (f): MMM(40%), and (h): BBPMS].

3.3. Mechanical Property Analysis.

As the gas separation membranes, they should have enough tensile strength and elongation at break during use. Figure 5 shows the test data on
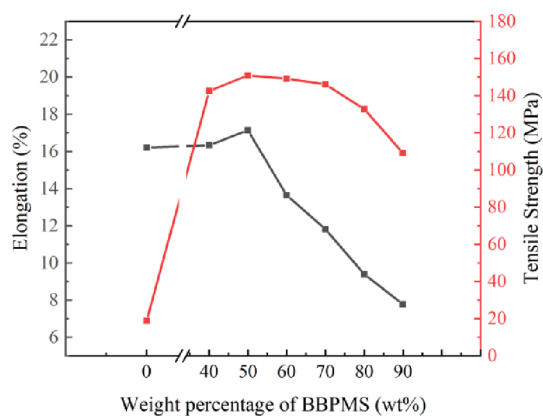

Figure 5. Mechanical properties of the EC/IL membrane and BBPMS/EC/IL membrane.

the tensile strength and elongation at break of the EC/IL membrane and BBPMS/EC/IL ternary composite membranes with membrane thicknesses between 117 and 136 μm. From Figure 5, it can be seen that the tensile strength and elongation at break of the composite membranes increased when the doping amount of BBPMS was 40 and 50% compared with the undoped membranes. The elongation at break and tensile strength of the composite membrane reached the maximum when the doping amount of BBPMS was 50%. When the doping amount of BBPMS exceeded 50%, the elongation at break and tensile strength started to decrease. In addition, with the increase of BBPMS doping, the elongation at break of the ternary composite membranes eventually became smaller than that of the EC/IL membrane. However, the tensile strength was always higher than that of the EC/IL membrane. This may be due to the increase of BBPMS doping, the silicon hydrogen bond in the polysiloxane breaks to form a hydrogen bond, and then the broken hydrogen bond combines with the −OH in the EC. The BBPMS/EC/IL hybrid membranes formed a kind of structure with interpenetrating networks.[31]

3.4. Thermal Property Analysis.

The thermogravimetric (TG) test plots of the EC/IL membrane and BBPMS/EC/IL ternary composite membrane are given in Figure 6. From Figure 6, it can be seen that the temperature at 5% weight loss
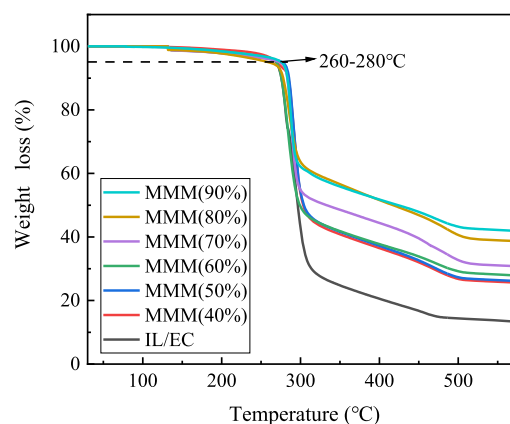

**Figure 6.** TG analysis of the EC/IL membrane and BBPMS/EC/IL membrane.

is in the range of 260−280 °C. With the increase of BBPMS doping, the weight loss temperature gradually increases, which is due to the fact that BBPMS is a cross-linked polymer whose thermal stability is better than that of EC. The residual amount of the mixed matrix membrane at 600 °C increased with the increase of BBPMS doping. The presence of BBPMS in a prepared hybrid matrix membrane was also demonstrated by the TG test.

3.5. Gas Separation Properties.

The prepared BBPMS/EC/IL ternary composite membranes were tested for the single component gas permeability of CO_2, N_2, and O_2, and the test data are shown in Table 2. According to the results in Table 2, the BBPMS complex membrane shows good gas transmission performance. CO_2 permeability of the BBPMS complex membrane is up to 1417.01 Barrer, O_2 permeability of the BBPMS complex membrane is up to 248.63 Barrer, and N_2 permeability of the BBPMS complex membrane is up to 97.12 Barrer. In contrast, its separation performance is not that good. The P_{CO_2}/P_{N_2} permselectivity values of the BBPMS membrane is 14.59 and the P_{O_2}/P_{N_2} permselectivity values of the BBPMS complex membrane is 2.56. Meanwhile, it can be seen that the gas permeability of the membranes gradually increased with the increase of the BBPMS doping amount, and the gas separability first increased and then gradually decreased. When the doping of BBPMS reaches 90%, the CO_2 permeation of the MMM(90%) membrane was 1806.03 Barrer, which is 20.04 times higher than that of the IL/EC membrane, which is due

Table 2. Gas Permeability, Gas Solubility, and Diffusivity Coefficients of BBPMS Complex Membrane, EC/IL Membrane, and BBPMS/EC/IL Membrane Measured (Single-Component Gas Permeability)

| no. | samples | $P_{(Bar)}$[a] | | | α | | S[b] | | | D[c] | | |
		CO_2	O_2	N_2	CO_2/N_2	O_2/N_2	CO_2	O_2	N_2	CO_2	O_2	N_2
1	MMM(90%)	1806.03	321.01	103.22	17.51	3.11	48.11	5.12	2.87	3.75	6.27	3.60
2	MMM(80%)	1034.09	208.03	55.32	18.72	3.76	26.52	3.99	1.24	3.90	5.21	4.46
3	MMM(70%)	585.99	124.82	30.73	19.14	4.07	14.23	2.50	0.97	4.13	4.99	3.16
4	MMM(60%)	405.98	76.05	20.23	20.09	3.76	10.20	2.21	0.69	3.98	3.44	2.94
5	MMM(50%)	350.06	46.53	13.10	26.73	3.55	8.52	1.45	0.57	4.11	3.21	2.31
6	MMM(40%)	212.09	29.42	10.44	20.39	2.83	6.25	1.32	0.39	3.39	2.23	2.69
7	IL/EC	90.10	16.71	3.83	23.52	4.36	3.12	2.01	0.11	2.89	0.83	3.39
8	BBPMS complex membrane	1417.01	248.63	97.12	14.59	2.56	30.44	4.56	2.14	4.66	5.45	4.54

[a]1 Barrer = 10^{-10} cm^3(STP) cm cm^{-2} s^{-1} $cmHg^{-1}$. [b]Ln 10^{-3} cm^3(STP) cm^{-3} $cmHg^{-1}$. [c]Ln 10^{-6} cm^2 s^{-1}.
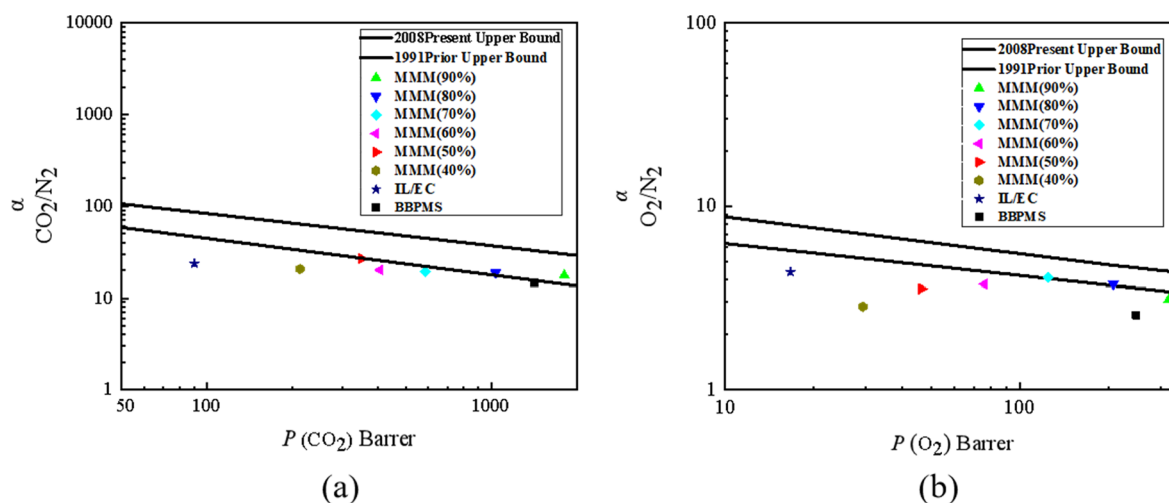
Figure 7. Plot of permselectivity vs permeability for the gas pairs (a) CO_2/N_2 and (b) O_2/N_2 (single component gas permeability).

Table 3. Gas Permeability, Gas Solubility, and Diffusivity Coefficients of the BBPMS Complex Membrane, EC/IL Membrane and BBPMS/EC/IL Membrane Measured (Mixed Component Gas Permeability)

| | | $P_{(Bar)}$[a] | | | | α | | S[b] | | | | D[c] | | | |
| | | CO_2/N_2 | | O_2/N_2 | | CO_2/N_2 | O_2/N_2 | CO_2/N_2 | | O_2/N_2 | | CO_2/N_2 | | O_2/N_2 | |
no.	samples	CO_2	N_2	O_2	N_2			CO_2	N_2	O_2	N_2	CO_2	N_2	O_2	N_2
1	MMM(90%)	1577.02	80.60	269.61	70.92	19.62	3.81	43.61	2.60	4.81	2.42	3.62	3.13	5.63	3.00
2	MMM(80%)	903.10	43.21	174.70	38.81	20.90	4.52	24.20	1.11	3.62	1.00	3.69	3.92	4.90	3.91
3	MMM(70%)	508.32	23.72	104.80	22.32	21.43	4.69	12.92	0.92	2.30	0.81	3.93	2.61	4.60	2.83
4	MMM(60%)	352.21	15.63	63.81	14.49	22.61	4.40	9.33	0.72	2.11	0.62	3.81	2.20	2.99	2.42
5	MMM(50%)	306.43	10.21	39.12	9.10	30.00	4.33	7.71	0.63	1.32	0.53	4.00	1.73	3.01	1.80
6	MMM(40%)	185.32	8.10	24.69	7.32	22.82	3.42	5.59	0.44	1.20	0.32	3.32	1.99	2.10	2.42
7	IL/EC	78.40	3.12	14.03	2.93	25.32	4.91	2.81	0.13	1.79	0.10	2.83	3.13	0.83	2.91
8	BBPMS complex membrane	1326.01	87.80	224.62	80.24	15.12	2.80	35.60	2.20	4.50	2.13	3.73	4.02	5.01	3.81

[a]1 Barrer = 10^{-10} cm^3(STP) cm cm^{-2} s^{-1} $cmHg^{-1}$. [b]Ln 10^{-3} cm^3(STP) cm^{-3} $cmHg^{-1}$. [c]Ln 10^{-6} cm^2 s^{-1}.

to the high gas permeability of the introduced BBPMS structure itself.[32] Combining the solubility and diffusion coefficients of CO_2, O_2, and N_2 gases listed in Table 2, it can be found that the CO_2 permeation was dominated by dissolution, and its solubility has a large increase with the addition of BBPMS, which also proved that the addition of BBPMS has shown great improvement in the CO_2 permeation. Generally, in the prepared BBPMS/EC/IL mixed matrix membranes compared to the prepared EC/IL membranes, the separation factor of CO_2/N_2 increases significantly and the O_2/N_2 separation coefficients are not very different. (The

calculation formula has been placed in the Supporting Information).

The gas permeation selectivity of the prepared ternary composite membrane was also compared with the Robeson curve.[30] CO_2/N_2 permeability of the BBPMS/EC/IL membranes were determined, and the results are shown in Figure 7a. When BBPMS were doped at 50, 70, 80, and 90%, the CO_2/N_2 capacity of the composite membrane exceeded the Robeson line of 1991. Especially, when the doping amount of BBPMS was 90%, the CO_2/N_2 capacity of the composite membrane has been closer to the Robeson line of 2008. The
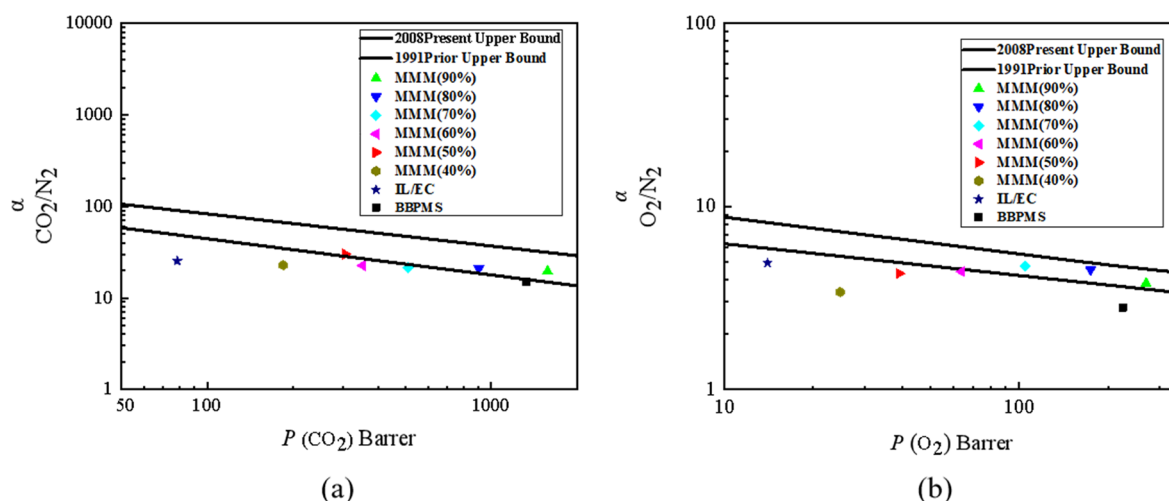
Figure 8. Plot of permselectivity vs permeability for the gas pairs (a) CO_2/N_2 and (b) O_2/N_2 (mixed component gas permeability).

O_2/N_2 permeability of the BBPMS/EC/IL membranes were also determined, and the results are shown in Figure 7b. When BBPMS were doped at 70 and 80%, the O_2/N_2 capacity of the composite membrane exceeded the Robeson line of 1991. When the doping amount of BBPMS was 90%, the O_2/N_2 capacity of the composite membrane has been closer to the Robeson line of 1991. All the above data show that this ternary composite membrane idea is successful.

The prepared BBPMS/EC/IL ternary composite membranes were tested for the mixed component gas permeability of CO_2/N_2 and O_2/N_2, and the test data are shown in Table 3. According to the results shown in Table 3, the BBPMS complex membrane shows good gas transmission performance. CO_2 permeability of the BBPMS complex membrane is up to 1326.01 Barrer, O_2 permeability of the BBPMS complex membrane is up to 224.62 Barrer, and the transmission amounts of N_2 in different gas mixtures are 87.80 (CO_2/N_2) and 80.24 (O_2/N_2), respectively. In contrast, its separation performance is not so good. The P_{CO_2}/P_{N_2} permselectivity values of BBPMS membrane is 15.12, and the P_{O_2}/P_{N_2} permselectivity values of the BBPMS complex membrane is 2.80. Meanwhile, it can be seen that the gas permeability of the membranes gradually increased with the increase of the BBPMS doping amount, and the gas separability first increased and then gradually decreased. When the doping of BBPMS reached 90%, the CO_2 permeation of the MMM(90%) membrane was 1577.02 Barrer, which is 20.12 times higher than that of the IL/EC membrane, which is due to the high gas permeability of the introduced BBPMS structure itself.[32] Combining the solubility and diffusion coefficients of CO_2/N_2 and O_2/N_2 gases in Table 3, it can be found that the CO_2 permeation was dominated by dissolution, and its solubility has a large increase with the addition of BBPMS, which also proved that the addition of BBPMS shows great improvement in the CO_2 permeation. Generally, in the prepared BBPMS/EC/IL mixed matrix membranes compared to the prepared EC/IL membranes, the separation factors of CO_2/N_2 and O_2/N_2 increase significantly. (The calculation formula has been placed in the Supporting Information).

The gas permeation selectivity of the prepared ternary composite membrane was also compared with the Robeson curve.[33] CO_2/N_2 permeability of the BBPMS/EC/IL membranes were determined, and the results are shown in Figure

8a. When BBPMS were doped at 50, 70, 80, and 90%, the CO_2/N_2 capacity of the composite membrane exceeded the Robeson line of 1991. Especially, when the doping amount of BBPMS was 90%, the CO_2/N_2 capacity of the composite membrane was closer to the Robeson line of 2008. The O_2/N_2 permeability of the BBPMS/EC/IL membranes were also determined, and the results are shown in Figure 8b. When BBPMS was doped at 70, 80, and 90%, the O_2/N_2 capacity of the composite membrane exceeded the Robeson line of 1991. When the doping amounts of BBPMS were 70 and 80%, the O_2/N_2 capacity of the composite membrane was closer to the Robeson line of 2008. All the above data show that this ternary composite membrane idea is successful.

4. CONCLUSIONS

The ternary composite membranes with different ratios of BBPMS/EC/IL were prepared based on the previous study of EC/IL hybrid matrix membranes. The composite membranes have good mechanical properties and can maintain less than 5% thermal weight loss at 260 °C. The prepared composite membranes showed great improvement in the permeability of CO_2 and O_2. The CO_2 permeation reaches 1806.03 Barrer at 90% doping of BBPMS, which is 20.04 times higher than that of the MMM(0%) membrane. O_2 permeation reaches 321.01 Barrer, which is 19.21 times higher than that of the MMM(0%) membrane. Moreover, when the doping of BBPMS is 70 and 80%, the O_2/N_2 permeation performance of the membrane exceeded the Robertson 1991 curve and closed to the Robertson 2008 curve.

In summary, the BBPMS/EC/IL ternary composite membranes exhibited excellent gas separation performance, thermal stability, and mechanical property, which made it have more potential as a gas separation material.

■ ASSOCIATED CONTENT

ⓢ Supporting Information

The Supporting Information is available free of charge at https://pubs.acs.org/doi/10.1021/acsomega.1c06259.

　　Equations for *P*, *α*, *D*, and *S*; molecular weight of BBPMS; small scale of SEM images of the EC/IL membrane and BBPMS/EC/IL mixed matrix membranes; contribution of the BBMPS structure itself to the improvement of permeability; TG analysis of the EC/IL

membrane and BBPMS/EC/IL membranes (30−100 °C); Brunauer−Emmett−Teller surface area measurements of IL/EC, MMMs, and BBPMS complex; and curves of time-lag (PDF)

■ AUTHOR INFORMATION

Corresponding Authors

Shuangping Xu − College of Materials Science and Engineering, Heilongjiang Provinces Key Laboratory of Polymeric Composite Materials, Qiqihar University, Qiqihar 161006, China; Email: 02228@qqhru.edu.cn

Hongge Jia − College of Materials Science and Engineering, Heilongjiang Provinces Key Laboratory of Polymeric Composite Materials, Qiqihar University, Qiqihar 161006, China; Email: jiahongge@qqhru.edu.cn

Jingyu Xu − College of Materials Science and Engineering, Heilongjiang Provinces Key Laboratory of Polymeric Composite Materials, Qiqihar University, Qiqihar 161006, China; Liaoning Key Lab of Lignocellulose Chemistry and BioMaterials, Liaoning Collaborative Innovation Center for Lignocellulosic Biorefinery, College of Light Industry and Chemical Engineering, Dalian Polytechnic University, Dalian 116034, China; ● orcid.org/0000-0002-6724-9623; Email: xjy951011@163.com

Authors

Wenqiang Ma − College of Materials Science and Engineering, Heilongjiang Provinces Key Laboratory of Polymeric Composite Materials, Qiqihar University, Qiqihar 161006, China

Da Liu − College of Chemical Engineering, Daqing Normal University, Daqing 163712, China

Mingyu Zhang − College of Materials Science and Engineering, Heilongjiang Provinces Key Laboratory of Polymeric Composite Materials, Qiqihar University, Qiqihar 161006, China

Yanqing Qu − College of Materials Science and Engineering, Heilongjiang Provinces Key Laboratory of Polymeric Composite Materials, Qiqihar University, Qiqihar 161006, China

Hailiang Zhou − College of Materials Science and Engineering, Heilongjiang Provinces Key Laboratory of Polymeric Composite Materials, Qiqihar University, Qiqihar 161006, China

Yushu Zhang − College of Materials Science and Engineering, Heilongjiang Provinces Key Laboratory of Polymeric Composite Materials, Qiqihar University, Qiqihar 161006, China

Xintian Wang − College of Materials Science and Engineering, Heilongjiang Provinces Key Laboratory of Polymeric Composite Materials, Qiqihar University, Qiqihar 161006, China

Wenwen Zhao − College of Materials Science and Engineering, Heilongjiang Provinces Key Laboratory of Polymeric Composite Materials, Qiqihar University, Qiqihar 161006, China

Complete contact information is available at:
https://pubs.acs.org/10.1021/acsomega.1c06259

Notes

The authors declare no competing financial interest.

■ ACKNOWLEDGMENTS

■ REFERENCES

(1) Shakoor, A.; Ashraf, F.; Shakoor, S.; Mustafa, A.; Rehman, A.; Altaf, M. M. Biogeochemical transformation of greenhouse gas emissions from terrestrial to atmospheric environment and potential feedback to climate forcing. Environ. Sci. Pollut. Res. 2020, 27, 38513−38536.

(2) Sarp, S.; Hernandez, S.; Chen, C.; Sheehan, S. W. Alcohol Production from Carbon Dioxide: Methanol as a Fuel and Chemical Feedstock. Joule 2021, 5, 59−76.

(3) D'Alessandro, D.; Smit, B.; Long, J. Carbon Dioxide Capture: Prospects for New Materials. Angew. Chem., Int. Ed. 2010, 49, 6058−6082.

(4) Qiu, S.; Xue, M.; Zhu, G. Metal-organic framework membranes: From synthesis to separation application. Chem. Soc. Rev. 2014, 43, 6116−6140.

(5) Zeng, S.; Zhang, X.; Bai, L.; Zhang, X.; Wang, H.; Wang, J.; Bao, D.; Li, M.; Liu, X.; Zhang, S. Ionic-Liquid-Based CO_2 Capture Systems: Structure, Interaction and Process. Chem. Rev. 2017, 117, 9625−9673.

(6) Jiang, L.; Roskilly, A. P.; Wang, R. Z. Performance exploration of temperature swing adsorption technology for carbon dioxide capture. Energy Convers. Manage. 2018, 165, 396−404.

(7) Reddy, M.; Ponnamma, D.; Sadasivuni, K. K.; Kumar, B.; Abdullah, A. M. Carbon dioxide adsorption based on porous materials. RSC Adv. 2021, 11, 12658−12681.

(8) Younas, M.; Rezakazemi, M.; Daud, M.; Wazir, M. B.; Ahmad, S.; Ullah, N.; Inamuddin, S.; Ramakrishna, S. Recent progress and remaining challenges in post-combustion CO_2 capture using metal-organic frameworks (MOFs). Prog. Energy Combust. Sci. 2020, 80, 100849.

(9) Baran, P.; Zarębska, K.; Czuma, N. CO_2 adsorption properties of char produced from brown coal impregnated with alcohol amine solutions. Environ. Monit. Assess. 2016, 188, 416.

(10) Amooghin, A.; Mashhadikhan, S.; Sanaeepur, H.; Moghadassi, A.; Matsuura, T.; Ramakrishna, S. Substantial breakthroughs on function-led design of advanced materials used in mixed matrix membranes (MMMs): A new horizon for efficient CO_2 separation. Prog. Mater. Sci. 2019, 102, 222−295.

(11) Gao, H.; Bai, L.; Han, J.; Yang, B.; Zhang, S.; Zhang, X. Functionalized ionic liquid membranes for CO_2 separation. Chem. Commun. 2018, 54, 12671−12685.

(12) Rochelle, G. T. Amine Scrubbing for CO_2 Capture. Science 2009, 325, 1652−1654.

(13) Bernardo, P.; Drioli, E.; Golemme, G. Membrane Gas Separation: A Review/State of the Art. Ind. Eng. Chem. Res. 2009, 48, 4638−4663.

(14) Liaw, D.-J.; Wang, K.-L.; Huang, Y.-C.; Lee, K.-R.; Lai, J.-Y.; Ha, C.-S. Advanced polyimide materials: Syntheses, physical properties and applications. Prog. Polym. Sci. 2012, 37, 907−974.

(15) Xiao, Y.; Low, B. T.; Hosseini, S. S.; Chung, T. S.; Paul, D. R. The strategies of molecular architecture and modification of polyimide-based membranes for CO_2 removal from natural gas-A review. Prog. Polym. Sci. 2009, 34, 561−580.

(16) Liu, Z.; Liu, Y.; Qiu, W.; Koros, W. J. Molecularly Engineered 6FDA-Based Polyimide Membranes for Sour Natural Gas Separation. Angew. Chem. 2020, 59, 14877−14883.

(17) Murtaza, G. Ethylcellulose microparticles: A review. Acta Pol. Pharm. 2012, 69, 11−22.

(18) Sanaeepur, H.; Kargari, A.; Nasernejad, B.; Amooghin, A.; Omidkhah, M. A novel Co^{2+} exchanged zeolite Y/cellulose acetate

mixed matrix membrane for CO_2/N_2 separation. *J. Taiwan Inst. Chem. Eng.* **2016**, *60*, 403−413.

(19) Najafi, M.; Sadeghi, M.; Bolverdi, A.; Chenar, M.; Pakizeh, M. Gas permeation properties of cellulose acetate/silica nanocomposite membrane. *Adv. Polym. Technol.* **2017**, *37*, 2043.

(20) Shakeel, I.; Hussain, A.; Farrukh, S. Effect Analysis of Nickel Ferrite ($NiFe_2O_4$) and Titanium Dioxide (TiO_2) Nanoparticles on CH_4/CO_2 Gas Permeation Properties of Cellulose Acetate Based Mixed Matrix Membranes. *J. Polym. Environ.* **2019**, *27*, 1449−1464.

(21) Arjmandi, M.; Pakizeh, M.; Saghi, M.; Arjmandi, A. Study of Separation Behavior of Activated and Non-Activated MOF-5 as Filler on MOF-based Mixed-Matrix Membranes in H_2/CO_2 Separation. *Petrol. Chem.* **2018**, *58*, 317−329.

(22) Deng, J.; Bai, L.; Zeng, S.; Zhang, X.; Nie, Y.; Deng, L.; Zhang, S. Ether-functionalized ionic liquid based composite membranes for carbon dioxide separation. *RSC Adv.* **2016**, *6*, 45184−45192.

(23) Luo, J.; Zhu, T.; Song, Y.; Si, Z. Improved permeability by incorporating polysiloxane in SBS block copolymers for CH_4/N_2 gas separation. *Polymer* **2017**, *127*, 52−65.

(24) Wang, S.; Li, X.; Wu, H.; Tian, Z.; Xin, Q.; He, G.; Peng, D.; Chen, S.; Yin, Y.; Jiang, Z.; Guiver, M. D. Advances in high permeability polymer-based membrane materials for CO_2 separations. *Energy Environ. Sci.* **2016**, *9*, 1863−1890.

(25) Zou, X.; Zhu, G. Microporous Organic Materials for Membrane-Based Gas Separation. *Adv. Mater.* **2018**, *30*, 1700750.

(26) Xu, J.; Jia, H.; Yang, N.; Wang, Q.; Yang, G.; Zhang, M.; Xu, S.; Zang, Y.; Ma, L.; Jiang, P.; Zhou, H.; Wang, H. High Efficiency Gas Permeability Membranes from Ethyl Cellulose Grafted with Ionic Liquids. *Polymers* **2019**, *11*, 1900.

(27) Davidovich-Pinhas, M.; Barbut, S.; Marangoni, A. G. Physical structure and thermal behavior of ethylcellulose. *Cellulose* **2014**, *21*, 3243−3255.

(28) Khan, F. Z.; Sakaguchi, T.; Shiotsuki, M.; Nishio, Y.; Masuda, T. Synthesis, characterization, and gas permeation properties of silylated derivatives of ethyl cellulose. *Macromolecules* **2006**, *39*, 6025−6030.

(29) Li, X.-G.; Kresse, I.; Springer, J.; Nissen, J.; Yang, Y.-L. Morphology and gas permselectivity of blend membranes of polyvinylpyridine with ethyl cellulose. *Polymer* **2001**, *42*, 6859−6869.

(30) Fraga, S. C.; Monteleone, M.; Lanč, M.; Esposito, E.; Fuoco, A.; Giorno, L.; Pilnáček, K.; Friess, K.; Carta, M.; McKeown, N. B.; Izák, P.; Petrusová, Z.; Crespo, J. G.; Brazinha, C.; Jansen, J. C. A novel time lag method for the analysis of mixed gas diffusion in polymeric membranes by on-line mass spectrometry: Method development and validation. *J. Membr. Sci.* **2018**, *561*, 39−58.

(31) Xu, S.; Ma, W.; Zhou, H.; Zhang, Y.; Jia, H.; Xu, J.; Jiang, P.; Wang, X.; Zhao, W. Preparation of butadiene-bridged polymethylsiloxane (BBPMS)/ethyl cellulose (EC) hybrid membranes for gas separation. *Eur. Polym. J.* **2021**, *157*, 110679.

(32) Merkel, T. C.; Bondar, V. I.; Nagai, K.; Freeman, B. D.; Pinnau, I. Gas sorption, diffusion, and permeation in poly(dimethylsiloxane). *J. Polym. Sci., Part B: Polym. Phys.* **2000**, *38*, 415−434.

(33) Robeson, L. M. The upper bound revisited. *J. Membr. Sci.* **2008**, *320*, 390−400.